Physica B 406 (2011) 3308–3312

Contents lists available at ScienceDirect

Physica B

journal homepage: www.elsevier.com/locate/physb

Crystal growth and dielectric, mechanical, electrical and ferroelectric characterization of n-bromo succinimide doped triglycine sulphate crystals

Chitharanjan Rai [a,b], K. Byrappa [c], S.M. Dharmaprakash [a,*]

[a] Department of Physics, Mangalore University, Mangalagangotri 574199, Karnataka, India
[b] Department of Electronics, Kalpataru First Grade Science College, Tiptur 572202, Karnataka, India
[c] Department of Geology, Mysore University, Manasagangotri 570006, Karnataka, India

ARTICLE INFO

Article history:
Received 27 November 2010
Received in revised form
14 May 2011
Accepted 22 May 2011
Available online 27 May 2011

Keywords:
Doping
X-ray diffraction
Seed crystals
Ferroelectric
Hardness
Hysteresis

ABSTRACT

Single crystals of triglycine sulphate (TGS) doped with n-bromo succinimide (NBS) were grown at ambient temperature by the slow evaporation technique. An aqueous solution containing 1–20 mol% of n-bromo succinimide as dopant was used for the growth of NBSTGS crystals. The incorporation of NBS in TGS crystals has been qualitatively confirmed by FTIR spectral data. The effect of the dopant on morphology and crystal properties was investigated. The cell parameters of the doped crystal were determined by the powder X-ray diffraction technique. The dielectric constant of NBS doped TGS crystal was calculated along the ferroelectric direction over the temperature range of 30–60 °C. The dielectric constant of NBSTGS crystals decrease with the increase in NBS concentration and considerable shift in the phase transition temperature (T_C) towards the higher temperature observed. Pyroelectric studies on doped TGS were carried out to determine the pyroelectric coefficient. The emergence of internal bias field due to doping was studied by collecting *P–E* hysteresis data. Temperature dependence of DC conductivity of the doped crystals was studied and gradual increase in the conductivity with the increase of dopant concentration was observed. The activation energy (ΔE) calculated was found to be lower in both the ferroelectric and the paraelectric phases for doped crystals compared to that of pure TGS. The micro-hardness studies were carried out at room temperature on thin plates cut perpendicular to the *b*-axis. Less doped TGS crystals show higher hardness values compared to pure TGS. Piezoelectric measurements were also carried out on 010 plates of doped TGS crystals at room temperature.

1. Introduction

Triglycine sulphate (TGS) crystals are the most suitable material for developing detectors for infrared radiation, environmental analysis monitors, earth observation cameras, astronomical telescopes, military systems and target faces vidicons based on the pyroelectric effects [1]. It is an extensively studied ferroelectric material with a typical ferroelectric phase transition at 49 °C [2]. The crystal is monoclinic with space group $P2_1$ and $P2_1/m$ below and above the Curie temperature, respectively. The spontaneous polarization takes place along the *b*-axis. All the three glycine groups I–III participate in the polarization reversal in TGS crystal. Considerable amount of work is done by several researchers to improve the quality and properties of the TGS crystal by doping the crystal with organic, inorganic and metal ions. The dopant added to the solution can enhance, suppress or stop the growth of the crystal completely. The dopant effect depends on its concentration, temperature and pH of the solution. The effects of dopants on the growth rate, quality of the crystals, habit of crystal growing, physical parameters, etc. have been the subject of many experimental studies [3–5]. Some of the dopants improved the pyroelectric coefficient, reduced the dielectric constant and hence helped in achieving good pyroelectric figure of merit. However, the tendency of the crystals to depolarize with time is a serious problem. Numerous studies have been reported on the minimization of the depolarization effects [6–9]. Significant amount of phosphoric acid in TGS crystal improved the pyroelectric coefficient and coercive field [10–13]. A few reports about the DC conductivity of l-alanine, nitro aniline and phosphoric acid doped TGS crystals are available [14,15]. Growth of triglycine sulphate crystals with new and large molecular dopants to tailor the properties so as to use the crystal for electrical applications is the study of current interest. The literature on the studies of TGS doped with n-bromo succinimide is not available. The present paper deals with the growth and characterization of n-bromo succinimide (NBS) doped TGS crystals.

---

[*] Corresponding author. Tel.: +918242287363.
E-mail addresses: raichitharanjan@gmail.com (C. Rai), smdharma@yahoo.com (S.M. Dharmaprakash).

0921-4526/$ - see front matter © 2011 Elsevier B.V. All rights reserved.
doi:10.1016/j.physb.2011.05.048

2. Experimental methods and materials

2.1. Crystal growth

Triglycine sulphate was synthesized at pH 2.5 using Analar grade glycine (Merck India) and sulphuric acid taken in the molar ratio 3:1. The purity of the TGS salt was enhanced by re-crystallizing the salt three times. The purified salt was used as a basic material for growing n-bromo succinimide doped TGS (NBSTGS) crystals. Now onwards the new doped crystal is referred to as NBSTGS. The TGS solution was prepared by dissolving TGS in double distilled water. Saturated solution of TGS doped with four different concentrations of (in the range of 1–20 mol%) n-bromo succinimide (Merck India) was prepared at 45 °C and filtered using sintered glass micro-fiber filter paper with porosity less than 2 μm. The filtered solution was poured into experimental vessels and was kept in a dust free chamber for slow evaporation at ambient temperature. After definite period of evaporation the solution became supersaturated and tiny crystals were nucleated. Defect-free seed crystals were taken out from the experimental vessels and tied with the help of fine human hair from the scalp. These seed crystals were slowly lowered in the saturated mother solution and allowed to grow in these experimental vessels to get the bulk crystals. Large numbers of crystals of various sizes were grown in a time period of 20–45 days.

2.2. Powder X-ray diffraction and FTIR measurements

Powder X-ray diffraction data of pure TGS and NBSTGS crystals were collected at room temperature using a BRUKER AXS D8 Advanced X-ray Diffractometer with Cu K_α (λ=1.5418 Å) radiation in the 2θ range from 20° to 70° at a scanning rate of 2° min^{-1} for the finely crushed powder. To confirm the presence of various functional groups in TGS and NBSTGS, Fourier transform infrared (FTIR) spectrum was recorded in the range 400–4000 cm^{-1} using a Shimadzu-8700 FTIR Spectrometer for the powder sample by the KBr pellet technique.

2.3. Dielectric measurements

The capacitance of the crystal sample was measured using a HP4194A impedance/gain phase analyzer by heating the sample at a rate of 1 °C/min using Metler hot stage FP90 over the temperature range 30–60 °C. The data collected was used to calculate the dielectric constant and transition temperature. Samples for capacitance measurements were prepared in the form of thin plate cleaved perpendicular to ferroelectric *b*-axis from the regions of the crystals away from the seed so that they contain no flaws. The cleaved samples were polished to get flat and smooth surface of thickness approximately 1.5 mm. The opposite faces were electroded with conducting silver paste. The sample preparation technique is discussed in detail [16]. Before conducting the electrical measurements the samples were kept at 60 °C for 24 h to remove any moisture present.

2.4. Pyroelectric current and DC conductivity measurements

Pyroelectric current and DC conductivity measurements were carried out in a two-terminal cell by mounting the samples in an unclamped condition. Pyroelectric current was measured over the temperature range of 30–60 °C using a Keithley 610C electrometer. The sample preparation and current measurement technique are discussed in detail [17].

Before conducting the DC conductivity measurements, the crystal samples were heated to 65 °C and maintained there for about an hour. Thereafter the leakage current was measured during the cooling run using a Keithley 610C electrometer with the application of a constant field of 0.12 kV/cm. The samples prepared for the capacitance measurement were also used for the DC conductivity studies.

2.5. *P–E* hysteresis measurements

The crystal surfaces cleaved perpendicular to the ferroelectric *b*-axis was used to examine the *P–E* hysteresis loops. The cleaved plates (0 1 0) were polished to get a smooth and parallel surface. The prepared sample for the study is now in the form of thin plate of surface area about 25 mm^2 and thickness 1.5 mm. The parallel (0 1 0) faces were electroded with conducting silver paste. The hysteresis measurements of the samples were carried out at room temperature using a computer controlled automatic *P–E* loop tester. While doing measurements the crystal sample is placed inside a silicone oil bath.

2.6. Piezoelectric and hardness measurements

The piezoelectric measurements for pure TGS and NBSTGS were carried out on 010 plates at room temperature using PM300 Piezotest, UK, at 100 Hz with the application of 0.5 N dynamic force. The samples were cleaved perpendicular to the *b*-axis and polished till the thickness was reduced to 1.5 mm. The surface area of the samples used in this study was approximately 25 mm^2. The opposite faces were electroded with conducting silver paste.

The micro hardness of the crystals of pure TGS and NBSTGS was measured at room temperature on the 010 plates with Clemax fully automatic digital micro-hardness tester fitted with a Vickers diamond pyramid indenter. Flat, parallel and polished surfaces cut perpendicular to ferroelectric *b*-axis (0 1 0) are used in the measurement.

3. Results and discussion

3.1. Crystal growth and morphology

Fig. 1 depicts the photograph of pure TGS and NBSTGS crystals. We have grown large numbers of crystal by suspending the seed crystals in doped TGS solution. Less than 20 mol% of dopant concentration is suitable for growing optical quality bulk crystals by suspending the seed crystals in the growth solution. The quality of the crystals was found to be poor at higher concentrations. Visible defects were observed around the seed crystal, as the crystal grew bigger. The concentration of the dopant in the growth solution has larger impact on the shape, size and quality of the crystals harvested. It is found that the *ac*-plane area is sensitive to the dopant concentration. This yields larger, 010 faces, which makes the crystal very suitable for IR applications. The crystals are transparent, colorless, non-hygroscopic and stable under ambient conditions.

3.2. Powder X-ray diffraction studies

Powder X-ray diffraction pattern of pure TGS and 20 mol% NBSTGS crystals are shown in Fig. 2. The peaks observed in the X-ray diffraction profiles for the pure TGS crystal matched well with the reported ASTM data (organic index to the powder diffraction file, Joint Committee of Powder Diffraction Standards (1967)). The unit cell parameters of the grown crystals of TGS and the literature values are compared [17]. The X-ray diffraction analysis shows that the monoclinic structure of the TGS crystal doped with different amounts of doping entities undergoes no

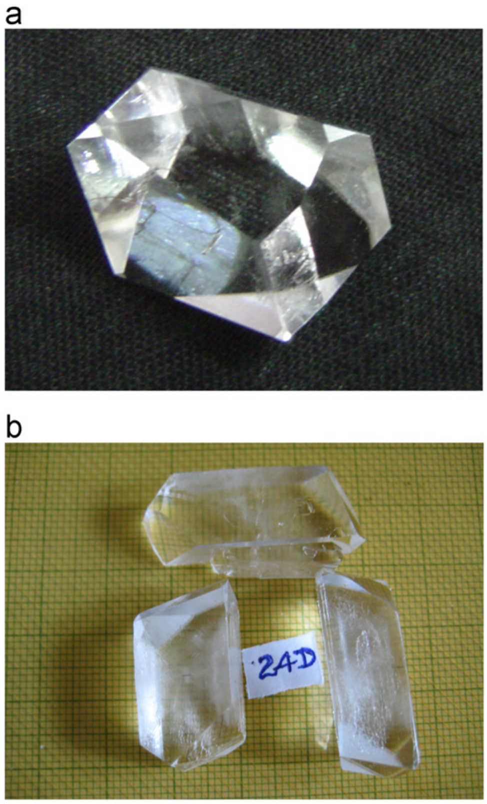

Fig. 1. (a) Pure TGS crystal and (b) NBSTGS (20 mol% doped) crystals.

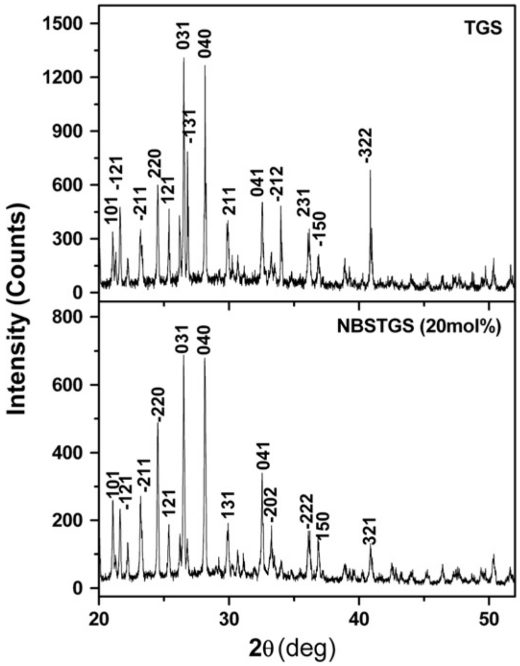

Fig. 2. Powder X-ray diffraction pattern of pure TGS and NBSTGS (20 mol% doped) crystals.

change. Despite low incorporation of dopant into the crystal lattice there is a significant change in the unit cell parameters of NBSTGS crystals. Lattice parameters of NBSTGS (20 mol%) $a=9.185$, $b=12.683$, $c=5.742$ and $\beta=105.46^{\circ}$ are found to be higher compared to those of pure TGS and the monoclinic angle β is found to decrease with the increase of dopant concentration.

3.3. FTIR studies

In order to analyze the presence of n-bromo succinimide qualitatively in TGS, the Fourier transform infrared spectra have been recorded for the powder sample by the KBr pellet technique. The FTIR spectra of pure TGS and NBSTGS (20 mol% doped) are shown in Fig. 3. The spectrum of TGS shows broad and strong absorption band in the range 2700–3600 cm^{-1} due to O–H stretching of hydrogen bonded carboxyl groups and the N–H stretching of NH_3^+ group. The C=O stretching vibration of carboxyl group displays its characteristic peak at 1685.7 cm^{-1}. The C–H bending vibrations appear at 1494.7 cm^{-1}. The peak present at 1413.7 cm^{-1} is assigned to N–H bending vibrations. The asymmetric and symmetric S=O stretching frequencies can be assigned to frequencies 1301.9and 1175 cm^{-1}, respectively. Stretching modes of carboxyl and sulphate ions are assigned to a strong band at 1126.4 cm^{-1}. The peaks appearing due to torsional oscillations of NH_3^+ group are seen at 619.1, 572.8and 501.5 cm^{-1}. The NBSTGS crystals also show a strong and broad absorption band due to O–H stretching of hydrogen bonded carboxyl groups and the N–H stretching of NH_3^+ in the range 2700–3600 cm^{-1} with a peak at 3114.8 cm^{-1}. This peak shifts towards higher wave number region as the dopant concentration is decreased. A new band appears at the frequency 1710.7 cm^{-1} in NBSTGS corresponding to C=O stretching vibration of carboxyl group of n-bromo succinimide. Some of the bands are narrowed in the spectra of the doped crystal, which is a clear indication of the presence of dopant in the TGS lattice.

3.4. Dielectric studies

The variation in dielectric constant of TGS and NBSTGS crystals is depicted as a function of temperature (30–60 °C) in Fig. 4. The phase transition temperatures were calculated by plotting inverse dielectric vs. temperature plot in the vicinity of the transition temperature and are presented in Table 1. It was observed that

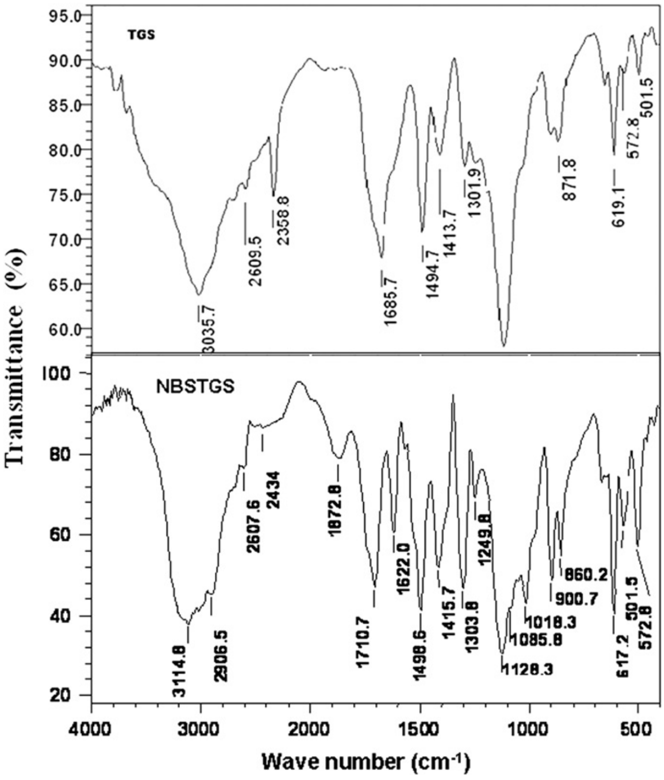

Fig. 3. FTIR spectra of pure TGS and NBSTGS (20 mol% doped) crystals.

the peaks of the dielectric curves are found to be suppressed and broadened with the increase of dopant concentration. This may be a clear indication of the presence of internal bias field in the crystals [18,19]. Similar behavior is also observed in dopants like iminodiacetic acid, alanine and urea. [16,20,21].

The doped crystals show smaller values of dielectric constant and higher ferroelectric transition temperatures compared to undoped TGS. The less doped crystals showing sharp peak as in like undoped TGS signifies that the crystal is homogeneous and strain free. The lowering of $\varepsilon'_{\max}$ and shifting of T_C to higher value may be due to the large sized NBS molecule, which goes substantially into the TGS lattice and replaces some of the glycine molecules.

The ε' value was found to decrease with increasing dopant concentration and also it decreased with increasing frequency. The dispersion observed in the dielectric constant in the low-frequency range may be attributed to an increase due to the presence of charged crystal defects [13], which is consistent with the observed increase in the DC conductivity of the doped crystals.

3.5. Pyroelectric studies

The direct method of Byer and Roundy [22] is used for the studies. Fig. 5 shows the temperature dependence of the pyroelectric coefficient for pure TGS and NBSTGS crystals; 1 mol% doped TGS shows slightly higher pyroelectric coefficient compared to pure TGS and the remaining samples studied show lower values of pyroelectric coefficient.

3.6. P–E hysteresis studies

The hysteresis loops observed for TGS and NBSTGS crystals are as shown in Fig. 6. The presence of internal bias field in the NBSTGS crystals is clearly observed in the P–E hysteresis loops. The measured values of maximum polarization (P_s^+) are 2.7, 2.11, 2.29, 2.0, and 2.27 μC/cm^2 for the TGS and 1, 5, 10 and 20 mol% NBSTGS crystals, respectively. The internal bias fields (E_b) are found to be zero for TGS and 0.65, 12, 21 and 3 kV/m for 1, 5, 10 and 20 mol% NBSTGS crystals, respectively, at room temperature. The maximum polarisation in case of the pure TGS is 2.7 μC/cm^2 and this value is very close to the value reported by Hoshino et al. [2]. The presence of internal bias field indicates that the dopant reduces the depolarizing effect in TGS crystals. The value of the internal bias field measured is maximum for 10 mol% n-bromo succinimide doped TGS crystals.

3.7. DC conductivity studies

DC conductivity of undoped TGS and NBSTGS crystals was determined in the temperature range 65–30 °C by applying a constant field of 0.12 kV/cm. The temperature dependence of the DC conductivity can be expressed as $\sigma_{DC}=\sigma_o \exp(\Delta E/k_B T)$, where k_B is Boltzman's constant, T is the absolute temperature, ΔE is the activation energy and σ_o is a constant. The variation of DC conductivity with the reciprocal of temperature (1000/T) of TGS and NBSTGS crystals is shown in Fig. 7. The DC conductivity at temperature 35 °C and activation energy in ferroelectric and paraelectric phases for TGS and NBSTGS crystals are presented in Table 1. For undoped TGS the value of DC conductivity is $5.5\times10^{-13}\ \Omega^{-1}\ \mathrm{cm}^{-1}$ and the activation energies in the ferroelectric phase of 1.42 eV and in paraelectric phase of 0.71 eV are observed. The values of DC conductivity and activation energies measured for undoped TGS are in good agreement with the earlier observations [14,15]. It was found that the conductivity of the doped crystals increased with the doping concentration both in ferroelectric and paraelectric phases. In the ferroelectric phase the

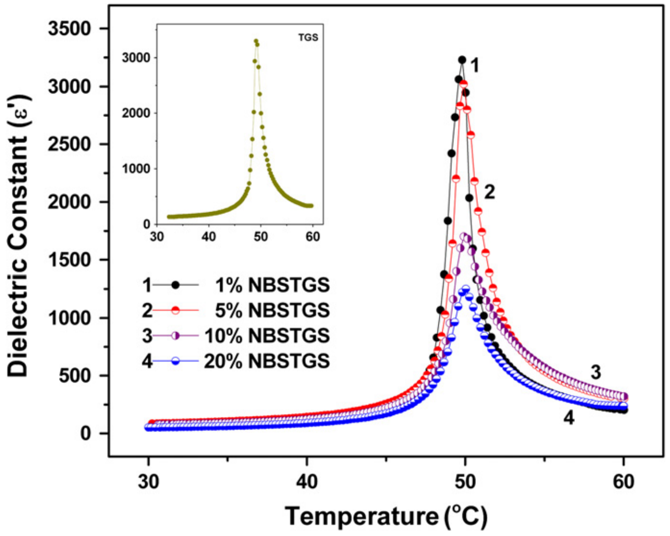

Fig. 4. Dielectric constant vs. temperature of NBSTGS crystals. Inset shows the temperature dependence of dielectric constant of pure TGS.

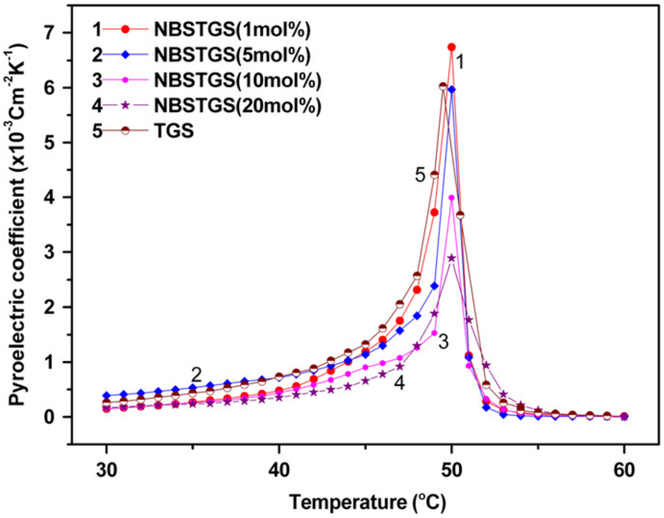

Fig. 5. Pyroelectric coefficient vs. temperature of pure TGS and NBSTGS crystals.

Table 1
Transition temperature, DC conductivity, activation energy, Vickers hardness number and piezoelectric coefficient of TGS and NBSTGS crystals.

Crystal	TGS	NBSTGS (1 mol%)	NBSTGS (5 mol%)	NBSTGS (10 mol%)	NBSTGS (20 mol%)
Transition temperature T_C (°C)	49.12	49.8	49.9	50.1	50.0
DC conductivity at 35 °C ($\Omega^{-1}\ \mathrm{cm}^{-1}$) $\times 10^{-13}$	5.55	9.87	11.49	14.08	16.25
Activation energy—ferroelectric phase (eV)	1.42	1.39	1.36	1.33	1.25
Activation energy—paraelectric phase (eV)	0.71	0.60	0.53	0.47	0.42
Vickers hardness H_V (kg/mm^2)	238	294	330	361	320
Piezoelectric coefficient d_{33} (pC/N)	41	34	42	41	53

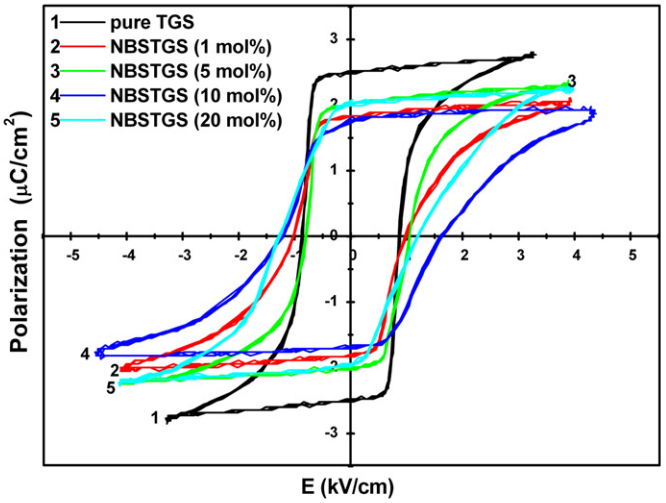

Fig. 6. Well-saturated hysteresis loops of pure TGS and NBSTGS crystals.

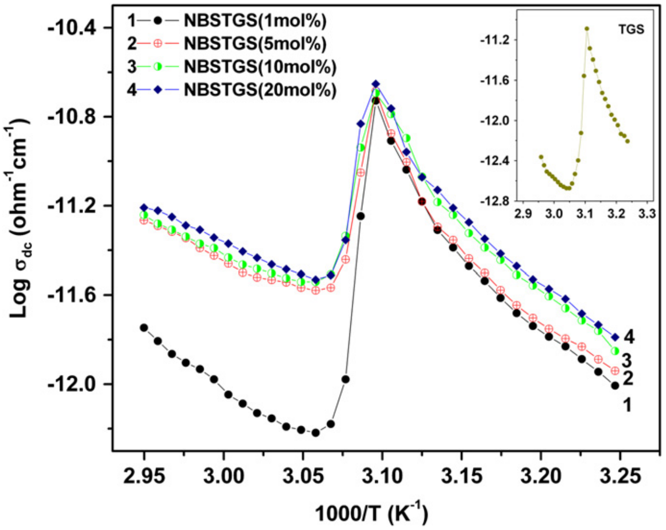

Fig. 7. Log σ_{DC} vs. 1000/T for pure TGS and NBSTGS crystals.

conductivity increased from 9.87 to 16.25 Ω^{-1} cm^{-1} at 35 °C and in paraelectric phase it increased from 17.9 to 61.9 Ω^{-1} cm^{-1} at 65 °C with the increasing dopant concentration from 1 to 20 mol%. The increase in conductivity of the NBSTGS crystals is the clear indication of the incorporation of the n-bromo succinimide dopant in the crystal lattice.

3.8. *Micro-hardness studies*

In the present investigation a Vickers indenter was used to measure the hardness of the crystal. The Vickers hardness is a measure of hardness of a material calculated from the size of an impression produced under load by a pyramid shaped diamond indenter. The micro-hardness is calculated from the relation $H_v = 1.8544P/D^2$ kg/mm^2, where P is the applied load and D^2 is the area of the indentation impression. The Vickers hardness for undoped TGS and NBSTGS crystals with doping concentration 1 –20 mol% with a load of 5 gm is presented in Table 1. The hardness values were found to increase for doped crystals compared to undoped TGS crystal. Increase in dopant concentration in NBSTGS crystals increases the hardness except for 20 mol% doped crystal. This may be due to the increased stress produced by the dopant molecules.

3.9. *Piezoelectric studies*

The d_{33} coefficient measurement was performed at room temperature on the poled samples using a piezometer at frequency 100 Hz with the application of 0.5 N dynamic force. The crystal samples were poled at an electric field of 1.5 kV/cm for an hour before the measurement of the d_{33} coefficient. The measured values of the d_{33} coefficient for pure TGS and NBSTGS crystals are presented in Table 1.

4. Conclusions

The NBS dopant has enhanced the growth in the *ac*-plane compared to pure TGS crystals; 1–10 mol% of dopant concentration is suitable for growing optical quality bulk NBSTGS crystals. The transition temperature is found to increase with the increase in dopant concentration. The dielectric and the *P–E* studies indicate the presence of internal bias field in the crystal, which is essential to prevent depolarization; 1 mol% doped crystals show slightly higher value of pyroelectric coefficient compared to pure TGS. DC conductivity studies reveal that the activation energy for the NBSTGS crystals is lower than that of pure TGS both in the ferroelectric and paraelectric phases with an enhancement in the DC conductivity. The dopant has enhanced the hardness of the crystals except for 20 mol% doped crystal. Not much variation is found in the piezoelectric coefficients. Based on the observed values of higher transition temperature, existence of internal field, lower dielectric constant and higher hardness number it is concluded that NBSTGS crystals are potential materials for pyroelectric detector applications.

Acknowledgements

C.R. is grateful to the University Grants Commission, New Delhi, for the award of teacher fellowship under FIP. The authors are thankful to Mr. Pramod Kumar Rai, CLCRI, Bangalore, for his help.

References

[1] V.V. Efimov, V.V. Ivanov, E.A. Klevtsova, N.N. Novikova, V.V. Sikolenko, S.I. Tiutiunnikov, E.A. Vinogradov, V.A. Yakovlev, Particles and Nuclei Letters 6 (115) (2002) 65.
[2] S. Hoshino, T. Mitsui, F. Jona, R. Pepnsky, Physical Review 107 (1957) 1255.
[3] R.J. Davey, E.A.D. White, Journal of Crystal Growth 30 (1975) 125.
[4] C.S. Fang, S.M. Dong, M. Wang, H.S. zhuo, M.H. Jiang, Journal of Crystal Growth 99 (1990) 891.
[5] K. Srinivasan, K. Meera, P. Ramaswamy, Crystal Research and Technology 35 (3) (2000) 291.
[6] P.J. Lock, Applied Physics Letters 19 (1971) 390.
[7] R.B. Lal, A.K. Batra, Ferroelectrics 142 (1993) 51.
[8] Chang-Shui Fang, Min Wang, Hong-Sheng Zhuo, Jian-Cheng Song, Ke-Cong Zhang, Ferroelectrics 142 (1993) 93.
[9] R. Murlidharan, R. Mohankumar, P.M. Ushasree, R. Jayavel, P. Ramasamy, Journal of Crystal Growth 234 (2002) 545.
[10] Yumin Kim, Gwangseo Park, Ferroelectrics 146 (1993) 99.
[11] N. Nakatani, M. Yoshio, Japanese Journal of Applied Physics 36 (1997) L425.
[12] Masakazu Yoshio Noriyuki Nakatani, Japanese Journal of Applied Physics 35 (1996) 5752.
[13] Vinay Gupta Aparna Saxena, K. Sreenivas, Journal of Crystal Growth 263 (2004) 192.
[14] S.C. Mathur, A.K. Batra, A. Mansingh, Journal of Physics D: Applied Physics 13 (1980) 79.
[15] Vinay Gupta Aparna Saxena, K. Sreenivas, Materials Science and Engineering B79 (2001) 91.
[16] Chitharanjan Rai, B. Narayana Moolya, S.M. Dharmaprakash, Physica B 406 (2011) 1.
[17] Chitharanjan Rai, K. Sreenivas, S.M. Dharmaprakash, Physica B 404 (2009) 3886.
[18] Genbo Su, Youping He, Hongzhi Yao, Zinkong Shi, Qingjin Wu, Journal of Crystal Growth 209 (2000) 220.
[19] M.E. Lines, A.M. Glass, Principles and application of Ferroelectric and Related Materials, Oxford University press, Oxford, 1977.
[20] G. Ravi, Anbukumar, P. Ramaswamy, Journal of Crystal Growth 133 (1993) 212.
[21] S. Aravazhi, R. Jayavel, C. Subramanian, Ferroelectrics 200 (1997) 279.
[22] R.L. Byer, C.B. Roundy, Ferroelectrics 3 (1972) 333.